CHAPTER II

MOLECULAR SIGNATURES OF ELECTROPOTENTIAL-INDUCED TRANSCRIPTIONAL SHIFTS IN *BACILLUS SUBTILIS*

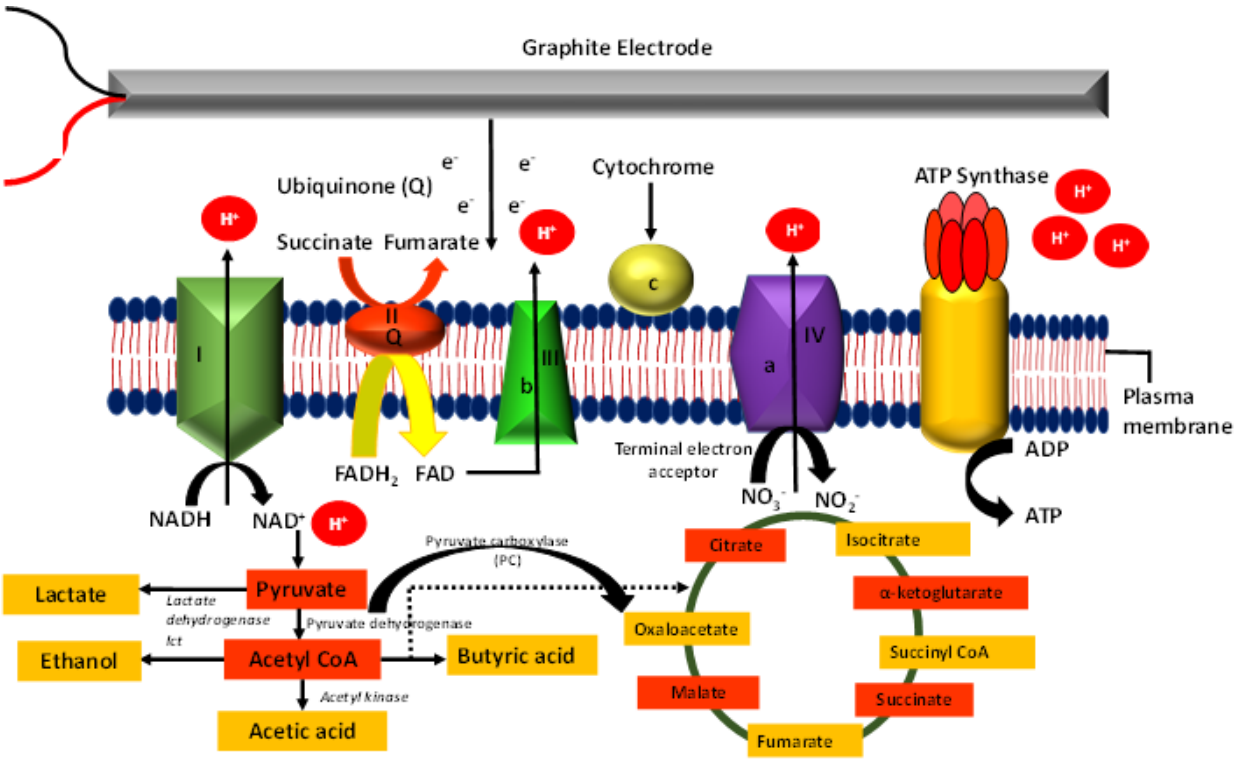

***Contents of Chapter 2.1 is published in the following peer-reviewed journals:**

1. **Mukherjee, T. and Venkata Mohan, S., 2021. Metabolic flux of Bacillus subtilis under poised potential in electrofermentation system: Gene expression vs product formation. *Bioresource Technology*, *342*, p.125854.**

CHAPTER II

Molecular Signatures of Electro-potential-Induced Transcriptional Shifts in *Bacillus Subtilis*

2.1 Introduction

Bacillus subtilis, a gram-positive bacterium, has several characteristics which includes the capacity to endure significantly lower pH, elevated temperatures, high sugar, salt, and a variety of other extreme conditions that might be used to build a robust bio-catalyst and strengthen the commercial competitiveness of biofuel and volatile fatty acids production (Nakano and Hulett, 1997; Romero et al., 2007; Chen et al., 2019; Kov'acs, 2019). *B. subtilis* is generally considered as innocuous; it can metabolise a vast array of carbohydrates and can successfully manufacture and deliver a wide range of value-added products (Kov´acs, 2019; Zhang et al., 2020; Kai, 2020; Romero et al., 2007; Ramos et al., 2000). External redox potentials stimulate the metabolic rates of bacteria in electro-fermentation systems (EF) by circumventing the thermodynamic redox restrictions imposed by internal redox disparity (Arunasri et al., 2020; Sravan et al., 2018). The external applied potential in an EF keeps the overall system in control via intracellular alterations by regulating the intrinsic redox balance comprising $NADH/NAD^+$(Arunasri et al., 2016, 2020; Chandrasekhar et al., 2021; Sravan et al., 2019; Vamshi Krishna and Venkata Mohan, 2019). Electrodes generate a redox potential gradient which leads to the metabolic alterations to produce products depending on the availability of electron donors and acceptors (Sarkar and Venkata Mohan, 2020; Sravan et al., 2020). In anaerobic conditions, some alternate electron acceptors partake in the electron transport chain other than oxygen (Vassilev et al., 2021; Ramos et al., 2000). Several researchers have documented the capacity of *B. subtilis* to utilize nitrate as an alternative electron acceptor (Clements et al., 2002; Ramos et al., 2000; Nakano and Hulett, 1997). A respiratory nitrate reductase (NarGHI) reduces nitrate to nitrite, which is then reduced to ammonia by a general cellular nitrite reductase during the anaerobic nitrate ammonification process (NasDE) (Clements et al., 2002; Ramos et al., 2000; Nakano and Hulett, 1997). The current work uses a facultative *B. subtilis* as a model organism in EF systems to better understand the connection between polarised redox potential and the corresponding metabolic processes. Pyruvate is a crucial intermediate component necessary for numerous metabolic processes and is the final product of glycolysis (Arunasri et al., 2020). In comparison to pyruvate, glucose is said to generate less organic acid since it creates multiple superfluous by-products, hence pyruvate

was chosen as a source of carbon in this study. Through pyruvate, *B. subtilis* generates lactate, acetate, butanediol, and traces of ethanol (Rahimi et al., 2020; Romero et al., 2007). It is also reported that with the addition of pyruvate as sole carbon source, the production of ethanol increases (Romero et al., 2007). Pyruvate dehydrogenase (*pdh*A), lactate dehydrogenase (*lct*E), and the pyruvate carboxylase (*pyc*A) are believed to be the primary pathways for pyruvate dissimilation in *B. subtilis* (Ramos et al., 2000). *pdh*A during fermentation, converts pyruvate to Acetyl CoA. Acetyl CoA leads to the production of acetate and ethanol, both of which contribute to the production of ATP and the maintenance of redox balance. Pyruvate is reduced to lactate and H^+ when *lct*E is active (Arunasri et al., 2020; Ramos et al., 2000). Further, pyruvate can also produce oxaloacetate with the aid of the enzyme pyruvate carboxylase (*pyc*A). OAA is an intermediate for TCA cycle, glycogenesis and aspartic acid synthesis (Nghiem et al., 2017). The goal of this research is to study the fate of the polarised redox potentials on EF of pyruvate and the resulting metabolic pathway alterations based on the expression of six enzymes namely lactate dehydrogenase, pyruvate dehydrogenase, acetate kinase, pyruvate carboxylase, adenylosuccinate lyase and acyl CoA dehydrogenase encoded by genes *lct*E, *pdh*A, *ack*A, *pyc*A, *pur*B and *acd*A respectively. A membrane-bound enzyme NADH dehydrogenase encoded by ndh which governs the electron transport and H_2 production was also studied for its relative expression using real-time PCR (q-PCR). The real time gene expression was monitored in *B. subtilis* under varied poised conditions and the relative expressions were calculated by the transcript levels of the counter condition. The gene expression patterns of the key enzymes involved in pyruvate metabolism was correlated with the product formation and bioelectrochemical analysis.

2.2. Experimental Methodology

2.2.1. Materials

All the chemicals (Analytical grade) were used further without any purification. NH_4Cl, $MgSO_4.7H_2O$, $CuCl_2.2H_2O$, $MnSO_4.H_2O$, $CoCl_2$, $ZnSO_4$, $CaCl_2.6H_2O$, $FeCl_3$, nutrient broth (NB) and sodium pyruvate were purchased from HiMedia.

2.2.2. Biocatalyst

Bacillus subtilis (*BS;* NCIM-5781) was revived from glycerol stock and maintained on Agar plates under aerobic conditions (Vamshi Krishna and Venkata Mohan, 2019). A single pure

colony was transferred from the Agar plate to the nutrient broth (NB) (200 mL) and incubated at 37ºC for 12 hours. The overnight cultures were back-diluted into NB media at a dilution of 1:100 and grown (250 rpm; 37 ºC) till an OD of 0.8 was reached prior to inoculating the EF reactors.

2.2.3 Experimental Details

Nine identical bench scale single-chambered EF setups were fabricated using borosilicate glass bottles, which exhibited a working volume/total volume of 0.08/0.1 L with a headspace of 0.02 L. The electrodes used were a graphite electrode (anode 2 cm,0.5 cm diameter, cathode 4 cm,0.5 cm diameter) and a reference electrode (vs Ag/AgCl, 3.5 M KCl). Designed synthetic media (Venkata Mohan et al., 2010) [NH_4Cl (2 g/L); $MgSO_4.7H_2O$ (0.01 g/L); $CuCl_2.2H_2O$ (0.01 g/L); $MnSO_4.H_2O$ (0.0025 g/L); $CoCl_2$ (5.6 mg/L); $ZnSO_4$ (28.6 mg/L); $CaCl_2.6H_2O$ (0.01 g/L) and $FeCl_3$ (0.0025 g/L)], supplemented with 0.5% (w/v) of pyruvate (5 g/L) as carbon source was used as electrolyte in EF system. The reactors were inoculated with *Bacillus subtilis* grown overnight in NB. The control was supplemented only with the designed medium and electrodes while other reactors were supplemented with designed media, electrodes and poised potential of both negative and positive potential ranging from 0.2 V, 0.4 V, 0.6 V and 0.8 V (vs Ag/AgCl) on working electrode (anode) by using a potentiostat-galvanostat system (Biologic VMP-3). All of the reactors were cleaned and sterilised at the start and end of each cycle and the full reactor procedure was repeated. To obtain data for biological replicates, the reactors were also run in three systems and cycles.

2.2.4 Selected Gene Expressions

Real-time PCR was used to examine the relative expression of the targeted genes in the study. The cDNA of *B. subtilis* was extracted from varied reactor conditions and used as a template to monitor the relative expression of genes, namely *pdh*A (pyruvate dehydrogenase), *lct*E (lactate dehydrogenase), *ndh* (NADH dehydrogenase), *ack*A (acetate kinase), *pyc*A (pyruvate carboxylase), *purB* (adenylosuccinate lyase) and *acd*A (acylCoA dehydrogenase), respectively. The RNA isolation/extraction from *B. subtilis* was performed using Sigma Gen Elute - Total RNA Purification kit with the manufacturer's protocol. The RNA was eluted into 30 µl of the elution buffer provided with the kit and the RNA concentration was measured (Nanodrop, thermo). 500 ng of the RNA from each sample was used for first-strand cDNA synthesis kit (PrimeScript, TaKaRa). For the RT-PCR reactions (10 ml), 2.5 pM primer and 2X SYBR Green

PCR Master Mix (TB green prime mix, TaKaRa) was used (Table 1). Template was pre-incubated at 50 °C for 2 min, denatured at 95°C for 10 min and annealed for 40 cycles under thermal conditions [95 °C (20 s) and 55 °C (30 s)]. Relative expression of genes was calculated by the ΔΔCt method, which was based on product cycle threshold (Ct) (Arunasri et al., 2020). Expression of 16S rRNA gene was used as an internal standard for RT-PCR. All values reported represented the mean of at least three independent experiments. All the primers used were designed using Prime3 primer design software.

Table 2.1: List of primers used for the study

SL.No.	Gene	Enzyme	Primers	Sequence
1.	*pdh A*	Pyruvate dehydrogenase	Forward	5'-CATGGTATTTACGCGTGTGC-3'
			Reverse	5'-ATGTCCGCGAGAGAAAAGAA-3'
2.	*lct E*	Lactate dehydrogenase	Forward	5'-AGCAAACCAAAAACCTGGTG-3'
			Reverse	5'-TATTCGCTCAGCATGAAACG-3'
3.	*nnr A*	NAD(P)H dehydratase	Forward	5'-GTACAGCAGGCAGTCGATCA-3'
			Reverse	5'-TCCTTTGCATATTCCGCTCT-3'
4.	*ndh*	NADH dehydrogenase	Forward	5'-TACGATGCGCTTGTTGTAGG-3'
			Reverse	5'-GATGTCAGCAAGCTCACCAA-3'
5.	*acd A*	Acyl CoA dehydrogenase	Forward	5'-TATGCAAAAGAGCGAAAGCA-3'
			Reverse	5'-CGTTACCTTCATCGCCGTAT-3'

2.2.5. Analytic Methods

A 20µL of filtered sample was injected (0.22 µm porosity) into a Rezex monosaccharide H+ (diameter: 300 X 7.8 mm; particle size: 5 µm, flow rate: 0.5 mL/h; wave length: 210 nm) equipped with a RID detector (210 nm) through which organic acids (acetate, lactate, succinate, ethanol etc.) were analysed in HPLC (Shimadzu LC20A). The mobile phase was milliQ water (pH 7). The peaks of the samples were compared to organic acid standards (all of which were generated at a concentration of 1g/L). With argon as the carrier gas, H_2 was analysed using a gas chromatography (GC; Agillent Technologies) fitted with a thermal conductivity detector (TCD; 1/8 x 2 m Heysep Q column). The injector and detector were both kept at 60˚C, while

the oven was isothermally maintained at 100˚C. Using a spectrophotometer (Molecular devises), the growth of *B. subtilis* in EF systems was studied at 24-h intervals. Potentiostat-galvanostat system (Bio-Logic-VMP-3) was employed to record voltammograms at a scan rate of 10 mV/s and in the scan range of +0.8 to −0.8 V vs. Ag/AgCl (3.5 M KCl) (Sravan et al., 2018).

2.2.6. Computational Analysis

Search Tool for Retrieval of Interacting Genes/Proteins (STRING v 11.5) was used to predict the functional relations among the genes *pdhA, ndh, pyc*A*, pur*B*, lct*E*, acd* A and *ack*A. The STRING analysis expresses the protein-protein interaction, the degree of influence of one gene upon other gene, the co-expression of genes and the loci and linkage of the genes respectively. From STRING analysis, the functional metabolic pathways for the studied genes can be annotated by the KEGG (Kyto Encyclopedia of Genes and Genomes) pathway analysis.

2.3. Results and Discussion

2.3.1 Growth Curve of *B. subtilis*

For four days, *B. subtilis* growth was studied in EF systems poised with both positive and negative polarised potentials of 0.2 V, 0.4 V, 0.6 V, and 0.8 V (Fig. 1.a). A reactor with no voltage (0 V) served as a control, and anaerobically growing cultures (without electrodes) were also evaluated for growth and other analyses at the same time. For four days, growth was evaluated, and no significant differences were seen between poised and non-poised controls. *B. subtilis* cells appear to be in a logarithmic growth condition in the EF system (Fig. 1a). The results also demonstrated that poised potentials had no effect on growth rate when compared to non-poised control systems, since growth without electrodes exhibited a significant rise in the cells after 24 h. After 72 h, the -0.8 V system had a somewhat greater OD at 600 nm than the other poised conditions, followed by the -0.4 V system. The growth of *B. subtilis* was not affected much but the rate of product formation varied with reactors. The initial pH was maintained at 7 but, gradually increased over time. The ameliorated theory behind this may be due to the conversion of calcium acetate crystals into calcite crystals during biofilm formation (Arnaoteli et al., 2021). The $CaCO_3$ can be formed by the influenced biologic mineralisation where EPS can play a role in nucleation site (Barabesi et al., 2007; Ferral-Perez et al., 2020).

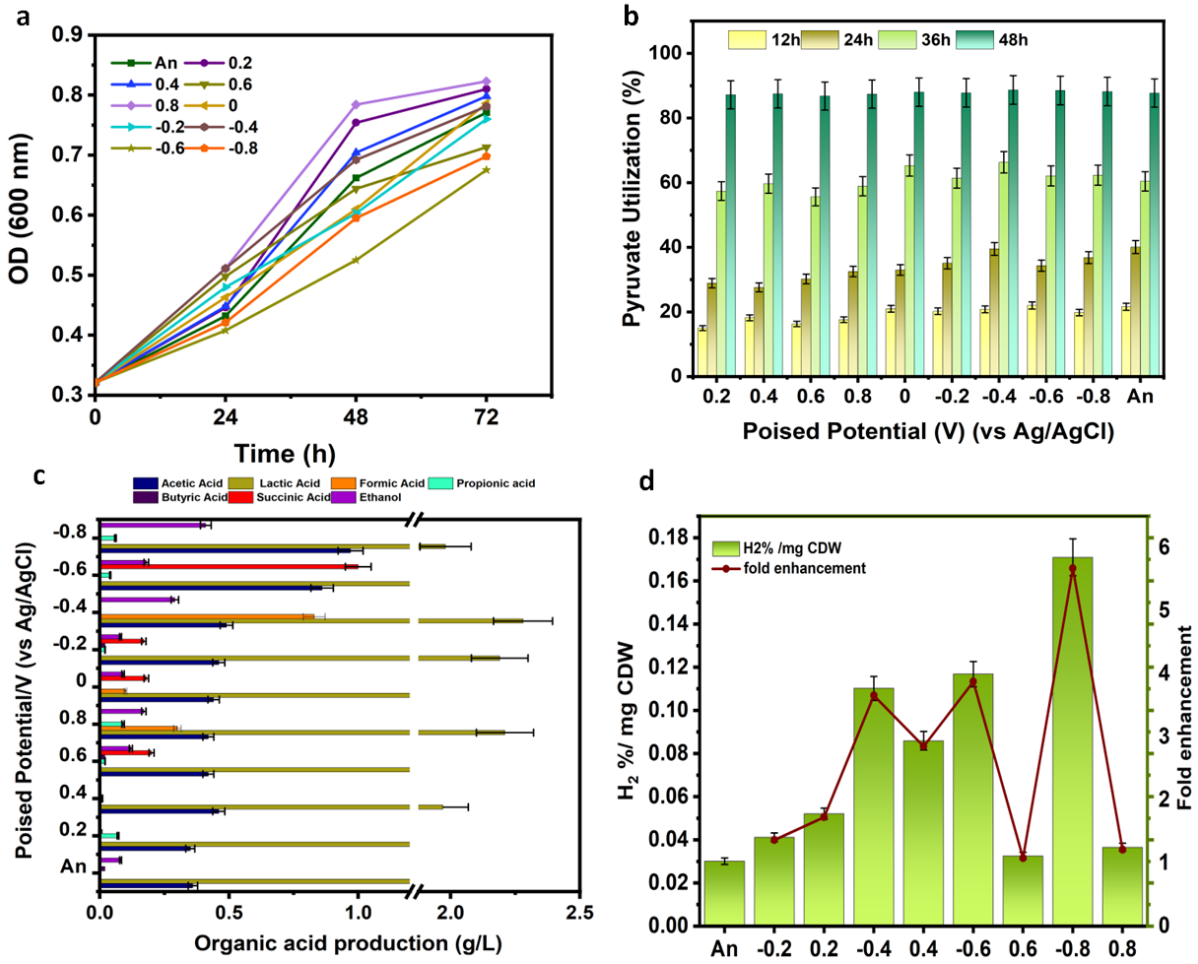

Fig. 2.1: Bioprocess Parameters. a). Growth curve of *B. subtilis* at different poised potentials/V (vs Ag/AgCl) conditions in *B. subtilis;* b). Pyruvate utilisation with respect to time at different poised potential/V (vs Ag/AgCl); c).Organic acids production at different poised potentials/V (vs Ag/AgCl) conditions in *B. subtilis*; d). Biohydrogen production and fold increment with respect to control under poised potential/V (vs Ag/AgCl) conditions in *B. subtilis* (An: Anaerobic, -0.2 V, -0.4 V, -0.6 V, -0.8 V, 0 V, +0.2 V, +0.4 V, +0.6 V, +0.8 V).

2.3.2. Pyruvate Utilisation

Pyruvate was used as a sole carbon source in all the reactors and with a gradual increment in time, the pyruvate consumption increased concurrently (Fig 2.1b). The maximum utilization was recorded by -0.4 V poised condition (89.1 %) followed by -0.8 V (88.5 %), -0.6 V (88.3 %), -0.2V (87.8 %), +0.4V (87.5 %), +0.8 V (86.8 %) and +0.2 V (87 %) with the least utilization efficiency by +0.6 (86.5%). The anaerobic control exhibited 87.9% utilization efficiency and 0 V reported 88 % removal efficiency. Overall, the pyruvate utilization efficiency can be demonstrated in the order as mentioned -0.4 V > -0.6 V > -0.8 V > 0 V > -

0.2 V > An > +0.4 V > +0.8 V > +0.2 V. This clearly depicts that more than 86.5 % pyruvate has been consumed by all the reactors at the end of 48 h cycle period and thus multiple products were generated concluding the efficient pyruvate metabolism.

2.3.3 Organic Acids

Improved production of several fatty acids with respect to time is reported in the current study. Formate, lactate, succinate, butyrate, propionate, acetate, and ethanol were found in samples taken from all reactors, including the control (anaerobic reactor) (Fig. 2.1c). In comparison to other poised and control settings, reactors poised with -0.6 V, -0.4 V, +0.8 V, and +0.4 V produced better proportion of lactate. Lactic acid was generated in almost all of the reactors which is apparently the major product in anaerobic fermentation (Eq. 2.1) followed by the acetic acid. The maximal lactate generation in these EF systems operated at -0.6 V (2.46 g/L) poised potential was roughly 50 %. Lactate concentrations were low when the reactor was set to +0.2 V potential. Lactate is formed when pyruvate is reduced by lactate dehydrogenase (*lct E*), which involves the simultaneous oxidation of one molecule of NADH for every molecule of pyruvate reduced. In reactors with -0.8 V (0.97 g/L), -0.6 V (0.86 g/L), and -0.4V (0.49 g/L), acetic acid was the most abundant organic acid generated (Eq. 2.2). Acetate can be generated by the expression of *ack*A gene (regulates the enzyme acetaldehyde kinase) which was subsequently high in reactors -0.8 V and -0.6 V respectively. Ethanol was observed maximum in -0.8 V (0.41 g/L) followed by -0.4 V (0.29 g/L) (Eq. 2.3). Ethanol is generally produced by the acetyl CoA which is in turn regulated by *pdhA* gene and NADH/NAD^+ ratio. Succinic acid (0.83 g/L) was observed maximum in +0.6V system. *pycA* and *purB* were reportedly high in the reactor +0.6 V which govern the formation of succinic acid. The negative poised potential favours the production of lactate, acetate and ethanol while positive potential favours succinic acid production.

$$Pyruvate + NADH \rightarrow Lactate + NAD^+ \quad \textbf{(2.1)}$$

$$AcetylCoA + Pi + ADP \rightarrow Acetate + HSCoA + ATP \quad \textbf{(2.2)}$$

$$AcetylCoA + 2NADH + 2H^+ \rightarrow Ethanol + HSCoA + 2NAD^+ \quad \textbf{(2.3)}$$

2.3.4 Biohydrogen

The synthesis of H_2 is the result of the metabolic conversion of organic substrates to acid metabolic intermediates in the form of short chain fatty acids or volatile fatty acids (Dahiya et al., 2015; Sravan et al., 2018; Sarkar et al., 2021). The generation of H_2 was measured in all

EF systems that were operated under poised circumstances as well as non-poised reactors. Compared to 0 V (control), all EF systems poised with electric potentials yielded relatively high H_2 production (Fig 2.1d). The range of H_2 increment ranged from 6-fold to 1.0-fold with respect to control. The resultant growth is in the order as-0.8 V (6-fold) > -0.6 V (4-fold) >-0.4 V (3.6-fold) > 0.4 V (2.8-fold) > 0.2 V (1.7-fold) > -0.2 V (1.3-fold) > -0.8 V (1.2-fold) > -0.4 (1-fold). The production of H_2 can infer that the electrons were utilised towards maintaining redox balance in the metabolic system (Sravan et al., 2018). H_2 production increased 6-folds at -0.8 V compared to the control followed by 4-folds with -0.6 V thus indicating the upregulation of hydrogenase complex and H_2 producing enzymes such as *ndh* (NADH dehydrogenase). This observation can conclude that NADH dehydrogenase enhances the metabolic flux and electron flux by increasing the NADH pool in the cell (Vamshi Krishna and Venkata Mohan, 2019). The NADH dehydrogenase enzyme is the most imperative enzyme in the interconversion of the substrate, which results in the production of protons and electrons. NADH dehydrogenase works in tandem with hydrogenase enzyme to transport proton across metabolic intermediates via redox mediators in an anaerobic microenvironment, eventually producing H_2 (Venkata Mohan and Linen Babu, 2011). The negative poised potential was more productive for hydrogen production due to the generation of more redox mediators. The associated gene (*ndh*) with H_2 production was also inferred to be more active when negative potential was subjected to the reactor.

2.3.5. Gene Expressions

Relative abundance of *pdhA* gene was plotted with respect to the reactor conditions (Fig 2.2.a). The higher potential relatively showed elevated expression of the *pdhA* compared to the lower potential. System operated with +0.6 V (10-fold) and -0.6 V (10-fold) resulted in highest *pdhA* expression while +0.4 V (0.7-fold) resulted in lowest. Acetate kinase favours the acetate formation via acetyl CoA and acetate phosphate as an intermediate. System operated with -0.8 V (6.7-fold) and -0.6 V (6.7-fold) resulted in highest *ackA* expression while +0.6 V (0.72- fold) resulted in the lowest. NADH dehydrogenase or *ndh* are strong electron donors and responsible for the generation of ATP in the electron transport chain. Apart from it, *ndh* enzyme is also responsible for several product formation in the metabolic pathway (Gyan et al., 2006). System operated with -0.8 V (4.6-fold) resulted in highest *ndh* expression while +0.4 V (0.5-fold) resulted in lowest. Highest lactate dehydrogenase (*lct*E) expression was higher in +0.8 V (15-

fold) and lowest in +0.2 V (1.4-fold). *pur*B replenishes the fumarate in the citric acid cycle which belongs to one of the three comprising the purine nucleotide cycle (Brosius and Colman, 2000). System operated with 0.8 V (1.5-fold) resulted in highest *purB* expression while +0.4 V (0.3-fold) resulted in lowest. *acd*A is associated with fatty acids biosynthesis pathway as well as controlling the long chain fatty acid production. System operated with +0.6 V (2.4-fold) resulted in highest *acd*A expression while -0.6 V (0.4-fold) resulted in lowest. *pycA* produces oxaloacetate from pyruvate and hence contributes in the TCA cycle. System operated with +0.8 V (4.3-fold) resulted in highest *pyc*A expression while -0.8 V (0.5-fold) resulted in the lowest.

The gene expression level with respect to enzyme activity was correlated with the product formation. The results depicted that -0.8 V had high *ndh* and *ack*A gene expression where H_2 and acetate are products. The *pdh*A was expressed good at -0.6 V, while *lct*E showed good expression at +0.8 V operations. The lactate production was regulated by the *lctE* gene whereas, the acetyl CoA synthesis was regulated by the *pdh*A expression. The lactate concentration in reactor with -0.6 V increased with the increment in the ratio of NADH/NAD^+ thus inferring that more the generation of NADH, more will be the lactate production (Farhana and Lappin, 2020; Vamshi Krishna and Venkata Mohan, 2019). The above statement can be correlated with the genes (*lct*E *and ndh*) encoding the lactate dehydrogenase and NADH dehydrogenase which were upregulated in the reactor -0.6 V, while downregulated in the reactor with +0.2 V (Fig. 2.3a). NADH dehydrogenase is a key component of the respiratory chain. It catalyzes the oxidation of NADH by transferring electrons to ubiquinone and establishes a proton motive force across the cell membrane (Gyan et al., 2006). *Bacillus subtilis* is a facultative aerobe that is capable of both aerobic and anaerobic respiration and has three predicted NADH dehydrogenases (*ndh, Yum*B*,* and *Yut*J) (Gyan et al., 2006). *ndh* is reported as an anaerobic gene regulating the electron transport as well as H_2 production (Gyan et al., 2006).

Pyruvate dehydrogenase belongs to the pyruvate dehydrogenase complex (PDHC), a group of enzyme complex which catalyses the production of acetyl CoA (an intermediate for several metabolic pathways) from pyruvate as a carbon source. PDHC generally contains three catalytic enzymes, two regulatory enzymes and a binding protein along with cofactors such as Thiamine pyrophosphate (TPP), lipolic acid and flavin adenine dinucleotide (FAD). Pyruvate dehydrogenase (E1), Dihydrolipoamide acetyltransferase (E2) and Lipoamide dehydrogenase

(E3) are the three enzyme components of PDHC. The initial enzyme in the PDHC is pyruvate dehydrogenase (E1) which undergoes the first step towards the transfer of acetyl CoA (Patel and Korotchina, 2003; Melkonian and Schury, 2019). The reactors with -0.6 V and -0.8 V have high *pdh*A expression which indicates the efficient production of acetyl CoA. Further, acetyl CoA produces acetate in two steps via acetyl phosphate with the expression of *ack*A gene. The reactors with -0.8 V and -0.6 V which showed higher acetic acid showed upregulation of genes *ackA* which regulates the production of acetate from the precursor acetyl CoA. The enhanced acetyl-CoA production through the upregulation of *pdh*A gene (Aristidou et al., 1999) produces acetaldehyde which in turn produces ethanol by the dissociation of NADH to NAD^+ which is a rate limiting step (Farhana and Lappin, 2020). Ethanol can also be generated by acetyl CoA subsequently by the acetaldehyde formation depending on the NADH/NAD^+ ratio. *acd*A is associated with fatty acids biosynthesis pathway. In *B. subtilis*, the degradation of long chain fatty acid is also associated with the *acd*A upregulation (STRING v 11.5). Thus, higher the *acdA* production, lower the chances of formation of long chain fatty acids (STRING v 11.5). From this study, it can be concluded that long chain fatty acids could be potentially synthesized from the negative poised condition (-0.2 V, -0.4 V, -0.6 V, -0.8 V) as it is having low concentration of *acd*A. While positive potential can lead towards more short chain and medium chain fatty acids respectively (0.2 V, 0.4 V, 0.6 V, 0.8 V).

Succinic acid will be produced in the presence of CO_2 associated with a suitable electron donor (Amulya and Venkata Mohan, 2021; Amulya et al., 2020). Supposition for the production of succinic acid is the catalytic activity of pyruvate carboxylase, an anapleuratic enzyme which is expressed by *pycA* gene. This gene accounts for the conversion of pyruvate towards oxaloacetate (OAA) that further gets transmuted to intermediate metabolic compound fumarate for the final production of succinate (Nghiem et al., 2017). Thus, both extreme poised potential conditions 0.8 V and -0.6 V that have upregulated *pyc*A can favor the formation of OAA through pyruvate that can lead to the production of succinate. *Pyc*A is reportedly found in *B. subtilis* but absent in enteric bacteria which utilises the phosphoenolpyruvate carboxylase for the conversion of phosphoenolpyruvate into oxaloacetate (Jitrapakdee et al., 2008). When *pyc*A gene is metabolically engineered in *E.coli* showed production of succinic acid through the key intermediate product OAA (Vemuri et al., 2002). The *pur*B gene encoding adenylosuccinate lyase enzyme can also be one of the reasons for the enhanced succinic acid production which is upregulated in the reactor with +0.6 V (Fig. 2.2.a). The *pur*B or

adenylosuccinate lyase is a member of the fumarase super family of metabolic enzymes in which fumarate is one of the end products through the cleavage of adenylosuccinate towards AMP and fumarate (Brosius and Colman, 2000). *purB* replenishes the fumarate in the citric acid cycle which belongs to one of the three comprising the purine nucleotide cycle (Brosius and Colman, 2000). This study founded that with the varied applied potentials, the gene expressions in the reactors enhanced with respect to the control reactor (0 V). Thus, poised potential can be considered as a potential candidate for the improved electron transfer intracellularly in *B. subtilis* along with the production of several value-added products.

2.3.6. Network Analysis

STRING analysis can be used as a tool to assess the gene/proteins of known protein-protein interaction. The system level understanding of cellular processes along with the structural, functional and evolutionary properties of proteins can be annotated from this computational tool. In *B. subtilis*, pyruvate metabolism under anaerobic condition leads to the production of several metabolic products such as acetic acid, lactic acid, ethanol, succinic acid and hydrogen as the major products. The genes *ndh, pdh*A*, ack*A*, pyc*A*, pur*B*, lct*E and *acd*A were subjected to computational prediction analysis for the enzymes NADH dehydrogenase, pyruvate dehydrogenase, acetate kinase, pyruvate carboxylase, adenylosuccinate lyase, lactate dehydrogenase and acyl-CoA dehydrogenase respectively. The predicted interaction network analysis suggested the involvement of these genes either in occurrence (phylogenetic profile) or in co-expression. *lct*E is the core key gene for the pyruvate metabolism that has regulatory function and controls the expression of other associated genes. Four functional pathways can be predicted with respect to the above associated genes namely pyruvate metabolism, de novo AMP biosynthetic process, fatty acid biosynthetic process and acetyl CoA biosynthetic process respectively (Fig 2.2b). The networking analysis infers that all the genes are responsible for organic metabolic process and has close interaction with each other. *pdh*A*, ndh, acd*A *and lct*E *(ldh)* are involved in the oxidation-reduction process. *pur*B is associated with the AMP biosynthetic pathway and purine metabolism. The *ack*A is associated with the acetyl CoA biosynthetic process. Additionally, *acd*A is associated with the beta oxidation of fatty acid and degrades the long chain fatty acid synthesis. The gene co-expression was higher in *pdh*A*, lct*E *and pyc*A which infers that the above three genes are envisaged to be associated in same

metabolic pathway i.e. pyruvate metabolism. The co-expression of *ndh* and *lct*E is also evident by the above computational analysis (Fig 2.2).

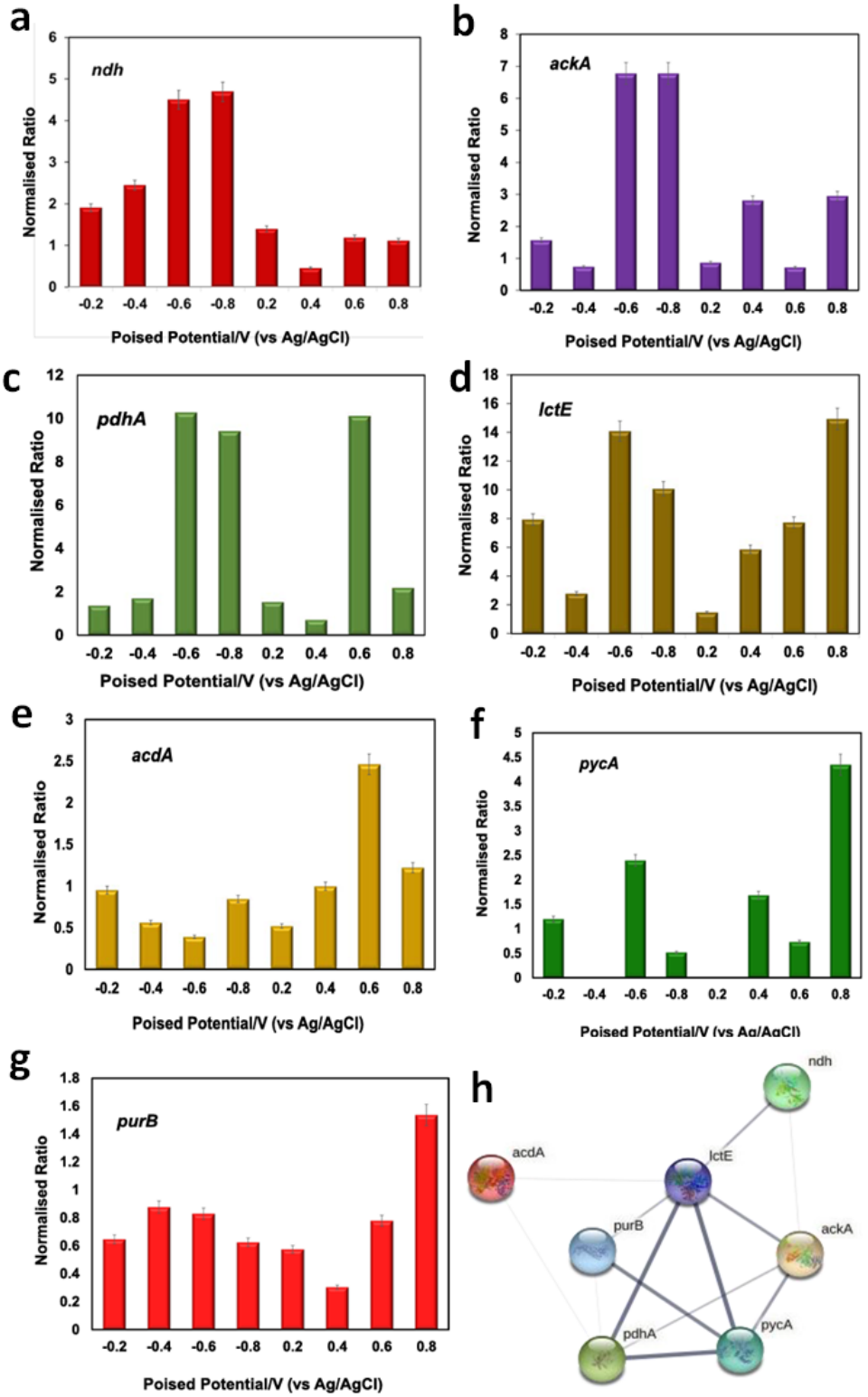

Figure 2.2: Relative expressions of genes (a) *ndh*, (b) *acdk*A, (c) *lct*E, (d) *pdh*A, (e) *acd*A, (f) *pyc*A, (g) *pur*B at different poised potentials/V (vs Ag/AgCl 3.5 KCl) conditions in *B. subtilis*, (h) Network interaction of genes depicted from STRING analysis

2.3.7. Bio-electrochemical Analysis

Voltammograms were recorded (10 mVs^{-1}) for all the reactors that were poised with different potentials (-0.8 V to +0.8 V) using working electrode as anode and counter electrode as cathode against reference electrode (Ag/AgCl (3.5 M KCl)) (Fig. 2.3). The oxidation and reduction peaks of a CV indicate the presence of an oxidant or a reductant in a redox process that was evaluated using conventional redox potentials (Modestra et al., 2020). The detected redox potential can also be used to measure metabolic state. Oxidases and reductases in *B. subtilis* participate in oxidation and reduction processes depending on the electron donor and acceptor affinity (Vamshi Krishna and Venkata Mohan, 2019). With the occurrence of various redox reactions, the current generation pattern was in line with the applied potential, which directs the metabolic pathway towards particular product formation (Guang et al., 2020; Arunasri et al., 2020). On voltammograms, different peaks were found for each experimental condition, indicating the existence of a redox mediator or a membrane associated redox protein involved in the electron transfer process. The peak potentials in all reactors were computed in relation to the Standard Hydrogen Electrode (SHE), which provided information on the electron transfer chain and change in metabolism of *B. subtilis* with respect to electrodes and applied potential (Fig 2.3; Table.2.2). The redox (oxidative/reductive) peak potentials observed in the reactors poised with different potentials against Ag/AgCl were observed to be positioned at -0.1 V/-0.2 V (-0.2 V reactor), -0.05 V/ -0.3 V, -0.6 V, -0.8 V (-0.4 V reactor), 0.3 V, 0.05 V/-0.8, -0.3 V (-0.6 V reactor), 0.05 V, 0.3 V/-0.3 V, -0.6V (-0.8 V reactor), 0.1 V/ 0.2 V, 0.5 V (+0.2 V reactor), 0.2 V/-0.5 V (+0.4 V reactor), 0.05 V/0.4 V (+0.6 V reactor) and 0.1 V/-0.2V (+0.8 V reactor) respectively. Quinones with different redox potentials link these oxidases and reductases. Fumarate reductase (-0.2 V vs. Ag/AgCl) and Iron reductase (0.5 V vs. Ag/AgCl) were found along with lactate dehydrogenase (-0.3 V vs. Ag/AgCl), based on peak potentials acquired from voltammograms. Cytochromes (a,c) (0.1 V and 0.05 V vs Ag/AgCl) responsible for the electron transfer was also reported. Acetate reductase (0.3 V vs. Ag/AgCl) for the generation of ethanol was also observed. The existence of pyruvate and lactate redox couple was detected in reactors poised with -0.6 V and -0.4 V, whereas acetate reductase, which mediates the generation of ethanol, was detected in reactors poised with -0.8 V and -0.6 V.

These findings imply that by channelling pyruvate to lactate and Acetyl Co-A, *B. subtilis* was restoring the intracellular redox equilibrium with $NADH/NAD^+$ ratio (Vamshi Krishna and Venkata Mohan, 2019). The NAD^+ readily accepts the electron to form NADH, therefore, more

the electron present, more the formation of NADH. Similarly, in the electron transfer chain, the NADH replenishes itself towards NAD^+ thus maintaining the NADH/NAD^+ pool. Thus, these results can conclude the rate of product formation in the reactor with -0.8 V and -0.6 V respectively. Supporting the above observation, the expression of *ndh gene* was also found high in the above reactors. The NADH is oxidised by pyruvate producing lactate, which is the major product of *B. subtilis* in general. Thus, it can be analysed the reason of getting lactic acid as a by-product which is subsequently high in reactors -0.6 V and -0.8 V. The indication of the cytochrome confirms that the electrons are channelised by this membrane protein towards electron transport chain thus enhancing the intracellular electron pool which is exhibited by all the reactors with poised potentials. The presence of FAD/$FADH_2$ in reactor with +0.4 V can conclude the production of succinic acid as FAD/$FADH_2$ is generated during the conversion of fumarate to succinate. FAD, a strong oxidising agent, when fully oxidised (quinone form) accepts two electrons and protons to transform into the hydroquinone form ($FADH_2$) (Ahmad et al., 2020). Flavins have multiple redox state which in turn helps in the transfer of electrons and H_2 which can be inferred for the reactor +0.4V, producing the highest H_2 among all the positive poised reactors. Apart from the role in the electron transport chain (complex III), it is also a potential candidate for the synthesis of several cofactors, such as heme CoA.

Table 2.2: Cyclic Voltammetry-based redox potential with respect to the applied poised potential

Potential/V (Ag/AgCl)	Redox peak potentials (against Ag/AgCl)	Reductase and Oxidase
0.2	0.1V; 0.2 V; 0.5V	Cyt a (red)/cyt a (oxi); NO_2^-/NO_3;Fe^{2+}/Fe^{3+}
0.4	0.2V; -0.5V	NO_2^-/NO_3^-; $FAD^+/FADH_2$
0.6	0.05V; 0.4V	Cytochrome c (red)/Cytochrome c (oxi), ATP Hydrolysis; MnO_2/Mn^{2+}
0.8	0.1V; -0.2V	Cyt a (red)/cyt a (oxi); fumarate/succinate
-0.2	-0.1V; -0.2V	Cytochrome b (red)/cytochrome b (oxi); fumarate/succinate
-0.4	-0.05V; -0.3V; -0.6 V; -0.8V	Ubiquinone oxi/ubiquinone red; Lactate/pyruvate; NAD^+/NADH; Pyruvate/CO_2
-0.6	0.3V;0.05V; -0.8V; - 0.3V	Acetyl CoA/Ethanol, $[Fe(CN)_6]^{3-}/[Fe(CN)_6]^{4-}$; Cytochrome c (red)/ Cytochrome c (oxi), ATP hydrolysis;Pyruvate/CO_2; Lactate/Pyruvate
-0.8	0.05V; 0.3V; -0.3V; -0.6V	Cytochrome c (red)/ Cytochrome c (oxi), ATP Hydrolysis; Acetyl CoA/Ethanol, $[Fe(CN)_6]^{3-}/[Fe(CN)_6]^{4-}$; Lactate/pyruvate; NAD^+/NADH

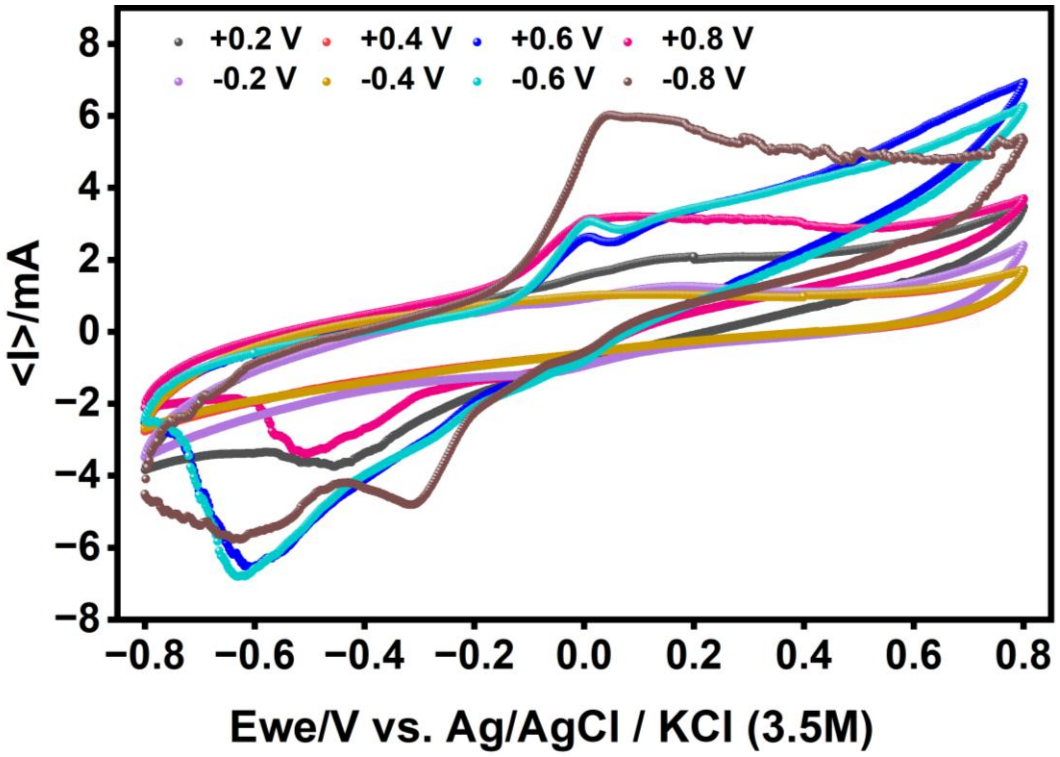

Figure 2.3: Bioelectrochemical analysis (Cyclic Voltammetry) Current vs Poised potentials/V (vs Ag/AgCl) conditions in *B. subtilis* (-0.2 V, -0.4 V, -0.6 V, -0.8 V, +0.2 V, +0.4 V, +0.6 V, +0.8 V)

2.3.8. Metabolic Flux Analysis-Poised Potential and Free Energy

Electron exchange in *B. subtilis* is explored in terms of on cellular redox and energy levels (Kracke et al., 2015). Intracellular electron transfer in *B. subtilis* results from the electron transfer mechanism initiating from NADH dehydrogenase (*ndh*) towards the membrane quinone followed by the surface-associated flavinylated PplA and finally to the terminal electron acceptor (nitrates, flavins, etc.) (Light et al., 2019). Electrons migrate through a range of electron transfer cofactors, such as flavins, iron-sulfur clusters, heme, and copper centers, as identified in the voltammograms, which are bound to integral membrane or membrane-associated protein complexes (Simon, 2013). The potential terminal electron acceptor for *B. subtilis* in anaerobic conditions was found to be NO_2^-/NO_3^- in cyclic voltammetry analysis (Table 2.2) which can be used to regenerate NAD^+ from NADH. The reduction of a terminal electron acceptor substrate is catalyzed by an appropriate redox enzyme and forms the final step of an electron transport chain serving in the generation of a proton motive force (pmf) across the membrane (Jorg Simon, 2013). The pmf is subsequently coupled to ATP synthesis according to Peter Mitchell's chemiosmotic theory (Jorg Simon, 2013).

The redox potential analysed from cyclic voltammetry clearly depicts that $NADH/NAD^+$ are strong electron donors (-320 mV) while NO_2^-/NO_3^- are strong electron acceptors (+430 mV). Thus, the consumption of NADH is more, the by-products formation will be less as it is involved in the transmembrane ion transfer thus maintaining a motive force that can initiate the ATP formation (Kracke and Kromer, 2016). The poised potential herein plays a major role in maintaining the electron pool by the microbial-electrode interaction. The difference in overall redox balance led to the transfer of electrons from extrinsic surface towards the intrinsic membrane (Bhagchandanii et al., 2020). The periplasmic protein, cytochrome, accepted the electrons and thus the electron transfer carries out in turn maintained the NADH pool which was auxiliary utilized for the formation of multifaceted by-products. Additionally, the energy required for the phosphorylation of ADP to ATP is supplied by electron flow in the electron transfer chain, where the difference in free energy ($\Delta G'_o$) between two adjacent redox carriers should be more than -9 kcal ($\Delta G'_o$= -n (0.023) $\Delta E'_o$, n= number of electrons) indicates that in a two-electron transfer, the difference in redox potentials at pH 7 and 25°C ($\Delta E'_o$) must be at least 220 mV (Konings and Boonastra, 1977; Kracke and Kromer, 2016).

The results from CV data show that difference in redox potential in the several electron donors and acceptors are sufficiently high for the synthesis of ATP. The direct electron transfer from the electrode and *B. subtilis* is more prominent due to the presence of the redox mediators (cytochrome, flavins) while the mediated electron transfer may also be reported due to the presence of potassium ferricyanide, quinones etc. (Pankratova et al., 2019). This reportedly assists in the enhanced electron and proton pool resulting in the more H_2 and value-added products formation (Pankratova et al., 2019). This correlates with the present study wherein the intermediate compounds ($NADH/NAD^+$, cytochrome) formed in the metabolic pathway of reactors -0.8 and -0.6 V resulted in the higher production of H_2. The presence of cytochrome indicates the channelisation of electrons mediated from the electrode towards inner membrane. The imbalance ratio of electrons was gradually sustained with the protons. The NADH replenished NAD^+ with the aid of the terminal acceptor, evidently NO^{2-}. The $NADH/NAD^+$ ratio was utilised further for the product formation wherein it plays a crucial role. The upregulation of lactate, ethanol and succinate can be potentially influenced by the upregulated $NADH/NAD^+$ as the ratio is associated directly for the formation of the afore mentioned products. Thus, the upregulated expression of *lct*E, *pdh*A, *pyc*A and *ndh* in the -0.8 V is indirectly governed by the upregulated $NADH/NAD^+$ ratio. The $FAD/FADH_2$ apart from

playing the crucial role in the electron transfer has a pivotal role in the TCA cycle and succinate metabolism. The presence of $FADH_2$ can simultaneously correlate with the upregulated *pur*B gene. This suggests that the metabolic pathways are regulated by the enzymes as well as the electron transfer mechanism which in turn regulates the production of the fatty acids and other biofuel. The external potential plays an important role in the enrichment of the electrons in the metabolic pathway of *B. subtilis.*

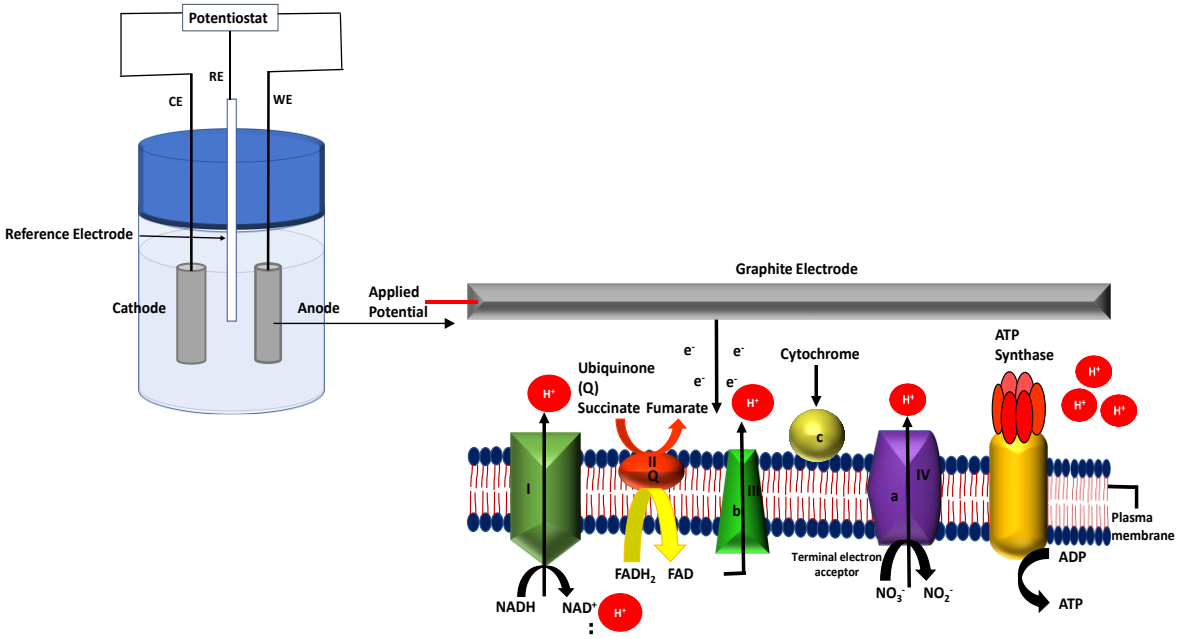

Figure 2.4: Proposed pathway of Pyruvate metabolism and anaerobic electron transfer in *B. subtilis* with respect to gene expression.

2.4. Conclusion

The poised potentials influenced the electron transfer as well as the expression levels of selected genes involved in pyruvate metabolism in *B. Subtilis*. The negative side of poised potential was more productive for H_2 as well as fatty acids. *lctE* gene encoding the lactate was found as core gene for pyruvate metabolism that regulates and controls the expression of other associated genes. The production of succinic acid was governed by *purB* (from formate) and *pycA* (from oxaloacetate) genes while the production of ethanol and acetate depends upon the expression of *pdhA* gene which regulates the activity of acetyl CoA.